ACI STRUCTURAL JOURNAL TECHNICAL PAPER

Title no. 89-S6

Shear Deformations in Reinforced Concrete Frames

by Frank J. Vecchio and Mohamed Basil Emara

Analytical procedures are described for considering the effects of shear on the deformation response of reinforced concrete frames. Presented also are the details and results of a corroborative test program involving a large-scale frame model. The theoretical and experimental investigations undertaken show that shear-related effects, through various direct and indirect means, can contribute significantly to frame deformation. Load capacity and failure mechanism can also be influenced. The analysis procedure is shown to provide fairly accurate predictions of these influences.

Keywords: deformation; frames; lateral pressure; loads (forces); **reinforced concrete; shear properties; shear tests**; stiffness; structural analysis.

A computer-based nonlinear frame analysis procedure (the computer program TEMPEST) was recently developed to predict the response of reinforced concrete plane frames subjected to thermal or mechanical loads.[1] The procedure was primarily based on performing rigorous sectional analyses of frame members at various points along their length, using appropriate stress-strain models, and then enforcing these sectional responses in the overall response of the frame. The influences of second-order effects such as material nonlinearity, geometric nonlinearity, time-and temperature-related effects, tension stiffening, and membrane action were intrinsically accounted for in the formulations.

The frame analysis procedure was found to predict fairly accurately the load-deformation response, load capacity, and failure mechanism of several test specimens.[2,3] In a test performed on a large-scale two-story frame model (Specimen BF1), however, it was observed that shear deformations were of sufficient magnitude to infuence significantly the frame's overall response.[4] The frame analysis procedure could not, at that time, account for shear-related influences and therefore underestimated the flexibility of the structure and did not correctly capture the final failure mechanism.

In a concurrent research program, analysis procedures were developed for predicting the response of beam sections subjected to combined shear, moment, and axial loads.[5] The analytical method developed (computer program SMAL) considered a layered representation of a beam cross section and applied the concepts and formulations of the modified compression field theory (MCFT)[6] in its analysis. In particular, the effects of concrete compression strain-softening and tension-stiffening were found to be critical factors in determining the response of a reinforced concrete beam section in shear. Corroboration with test data showed the procedure to be capable of predicting accurately the load-deformation and ultimate strength of beam sections.[5]

It thus became a research objective to adapt the successful beam section analysis procedure into the frame analysis algorithm, thereby incorporating the influence of shear-related effects. As well, additional experimental work would be undertaken to better understand the magnitude and influence of shear deformations in frame structures. This paper describes both the analytical developments and the results of the test program.

RESEARCH SIGNIFICANCE

Shear deformations in a frame structure can be significant and thus can be of practical importance in the design or behavior analysis of the structure. In the columns of a frame subjected to sidesway, for example, the added flexibility derived from shear deformations can add significantly to the computed secondary moment effects and can cause substantial redistribution of shear forces.

This paper, through both analytical and experimental investigation, gives an indication of the magnitude and relative significance of shear deformations. Methods by which these deformations can be predicted are also provided.

ANALYSIS PROCEDURES

The influence of shear can be incorporated into a nonlinear frame analysis algorithm by implementing layered sectional analysis procedures which consider two-dimensional stress conditions. In this work, the

ACI Structural Journal, V. 89, No. 1, January-February 1992.

Received Aug. 3, 1990, and reviewed under Institute publication policies.

ACI member **Frank J. Vecchio** *is an associate professor of civil engineering at the University of Toronto. A member of ACI Committees 435, Deflections of Structures; and 447, Finite Element Analysis, his research interests relate primarily to the constitutive modeling, nonlinear analysis, and computer-aided design of reinforced concrete.*

ACI member **Mohamed Basil Emara** *is a graduate student at the University of Toronto in the Department of Civil Engineering. He received his BSc from Cairo University, Cairo, Egypt, in 1986 and his MASc from the University of Toronto in 1990. He is currently working on his PhD in structural engineering at the University of Toronto. His interest areas include nonlinear analysis and the response of structures to seismic loading.*

analysis procedures previously developed and described for beam sections[5] will be directly coupled with the nonlinear frame analysis algorithm developed independently.[1]

A layered section analysis procedure can be used to model effectively the response of a beam cross section to general shear, moment, and axial forces. In this procedure, the member cross section is discretized into a series of concrete layers and longitudinal steel elements [see Fig. 1(a)]. The concrete layers and reinforcing steel elements are then decoupled and analyzed individually, although conditions of compatibility and equilibrium must be satisfied for the section as a whole. The only sectional compatibility requirement enforced is that plane sections remain plane. Sectional equilibrium requirements include a balancing of the horizontal shear flows as well as of the member end actions. Beyond this, uniform stress conditions are assumed to exist in each layer and each element. Conditions of compatibility and equilibrium in each concrete layer are enforced according to the formulations of the modified compression field theory.[6] The associated modeling and solution procedures are discussed in Reference 5. In this work, the shear forces acting on the cross section are treated according to the constant shear flow assumption, which was shown to give generally good results.[5]

Given the sectional forces, the two-dimensional stress and strain conditions within each layer of the section can be computed. The overall deformation reponse of the beam section will be defined by a longitudinal strain gradient and a shear strain distribution through the depth [(see Fig. 1(b)]. The response can be summarized by defining the section's curvature ϕ, axial strain at middepth ϵ_c, and average normal shear strain γ_a. The average shear strain is the average of the values determined for each layer. Because two-dimensional analyses are being performed for each layer, this approach will henceforth be referred to as the "multi-layer" analysis.

The deformation response of a frame member, computed at various sections along its length, can then be introduced into a nonlinear frame analysis by enforcing sectional strain compatibility. This can be done by various means; for example, by defining effective sectional stiffness factors, unbalanced forces, fixed end forces, or combinations of these. In the computer program TEMPEST, the shear deformations were incorporated by defining shear compatibility fixed-end forces, as given in Fig. 1(c). The axial and flexural deformations, the influence of shear forces on these deformations, and the overall frame analysis algorithm were modeled in the manner previously documented in Reference 1.

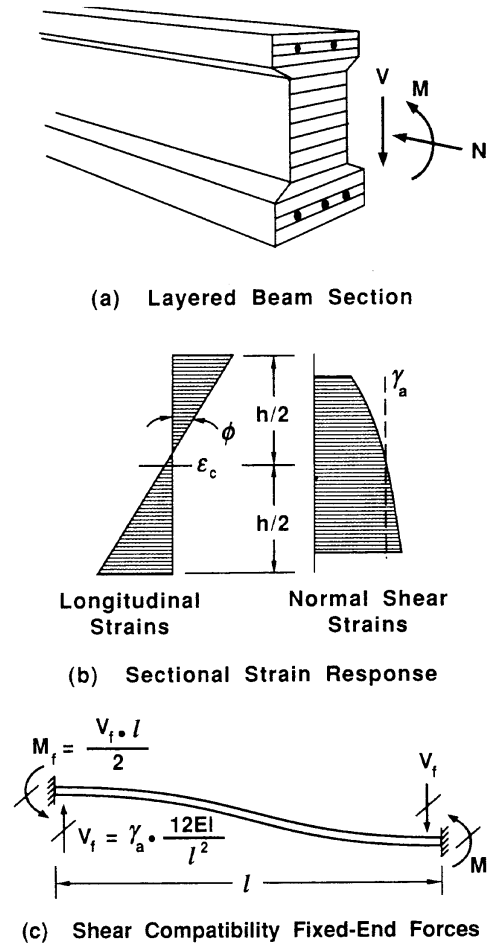

Fig. 1 — Modeling shear effects in frame members

The multilayer sectional analysis, when combined with the nonlinear frame analysis algorithm, results in a rather computation-intensive procedure. Thus, two alternative approximate procedures were implemented in an effort to reduce the computational demands. These alternative procedures can be referred to as the "single-layer" approach and the "modified-layer" approach.

In the single-layer approach, a two-dimensional stress analysis based on MCFT formulations is performed for the middle layer of the section only. The shear strain computed for this layer is taken to represent the average for the beam section. All the other layers are analyzed using uniaxial stress-strain relations, neglecting shear influences. Thus, the influence of shear on the axial and flexural deformation of the section is not considered.

In the modified-layer approach, the two-dimensional MCFT analysis is again performed for the middle layer only. And again, the shear strain computed is taken as the average value for the beam section. However, the strain-softening effect found in the middle layer, as a result of the shear stresses, is represented in terms of a

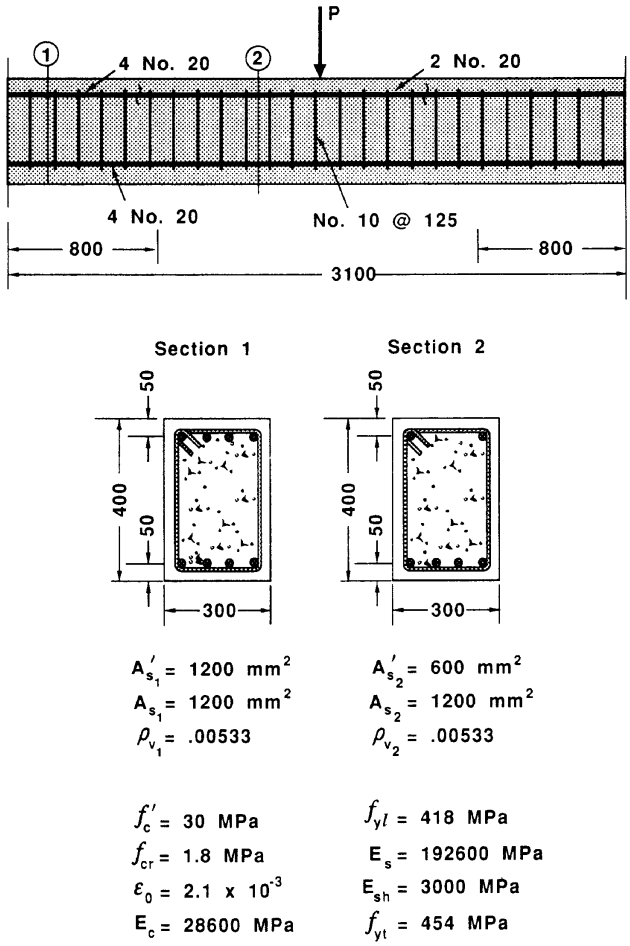

Fig. 2 — Details of beam specimen for theoretical study

correction in the longitudinal stress in the concrete. This stress correction is then uniformly applied to the stresses in each of the other layers computed using uniaxial stress-strain relations. Thus, the influence of shear on the axial and flexural stiffness of the section is approximately accounted for. This approach was first introduced, and is more fully described, by Adebar.[7]

THEORETICAL STUDY

To illustrate the influence of shear forces on the computed response of a reinforced concrete frame structure, the beam shown in Fig. 2 was examined. [This beam was part of test model BF1 (Reference 4).] The 3100 mm (10 ft, 2 in.) long beam is 300 mm (12 in.) wide by 400 mm (16 in.) deep, and is reinforced with four No. 20 bars as bottom reinforcement. Top flexural reinforcement is comprised of four No. 20 bars near the support regions, and two No. 20 bars in the midspan region. Shear reinforcement consists of No. 10 closed stirrups at 125 mm (5 in.) spacing. The concrete has a compressive strength of 30 MPa (4350 psi), a tensile strength of 1.8 MPa (260 psi), and a modulus of elasticity of 28,600 MPa (4150 ksi). Other pertinent details are provided in Fig. 2.

The beam was considered to be subjected to a concentrated load at the midspan. Analyses were conducted assuming that the beam was: a) simply supported at the ends, and b) fully fixed against translation and rotation at the ends. For each case, load-deformation response curves were computed using all of the alternative procedures discussed for considering shear force effects (i.e., multi-layer, modified-layer, and single-layer approaches), as well as by considering shear to be negligible.

The computed sectional responses for the two beams are given in Fig. 3. The local strain conditions shown for the simply supported beam correspond to a section at the midspan. For the fixed-end beam, the local strain conditions shown correspond to a section at the support. The overall response of the beams is described in Fig. 4 in terms of axial elongation, restraint force at the supports, and midspan deflection.

Shear stresses will contribute to the cracking of concrete and hence can be expected to result in the softening of a member's flexural stiffness. In the two beams analyzed, the influence of shear on the computed sectional curvatures is seen to be small but not negligible [see Fig. 3(a)]. At moderate load levels, shear is seen to cause about a 5 to 10 percent increase in the curvatures computed. The modified-layer procedure resulted in a predicted response very similar to that obtained from the multi-layer analysis. The response predicted using the single-layer procedure is essentially identical, as expected, to that obtained if shear is not considered.

The truss-like mechanism of shear resistance developed within a reinforced concrete beam relies on the longitudinal reinforcement to act as a tension chord. The additional tensile forces developed in the longitudinal reinforcement, due to shear, act to increase the axial expansion of the beam section. This is evident in the computed responses seen in Fig. 3(b), which describes the longitudinal strain at the middepth of the beam sections. Once again, the influence of shear is seen to cause a small but not inconsequential increase in strain. In the simply supported condition, the modified-layer response closely approximates that obtained using the more rigorous multi-layer method. In the case of the fixed-end beam, however, the modified-layer method appears to be sensitive to the high axial compressions induced in the beam and hence, shows more variation. The single-layer procedure, in this aspect of behavior, is little different than ignoring shear altogether.

Of primary interest are the computed transverse shear strains, shown in Fig. 3(c). Here, the variations in computed response are more pronounced. For the case of the simple beam, the single-layer procedure results in computed shear strains that are about 50 percent of the values obtained using the multi-layer analysis. The disparity results form an inability to account for rapidly increasing shear strains in layers near the tensile face, which lead to an average shear strain for the section generally greater than the value computed from conditions at the middepth. In the case of the fixed-end beam, the more rapidly increasing axial compressive force reverses this tendency. In both cases, the modified-layer procedure gives slightly higher shear strains,

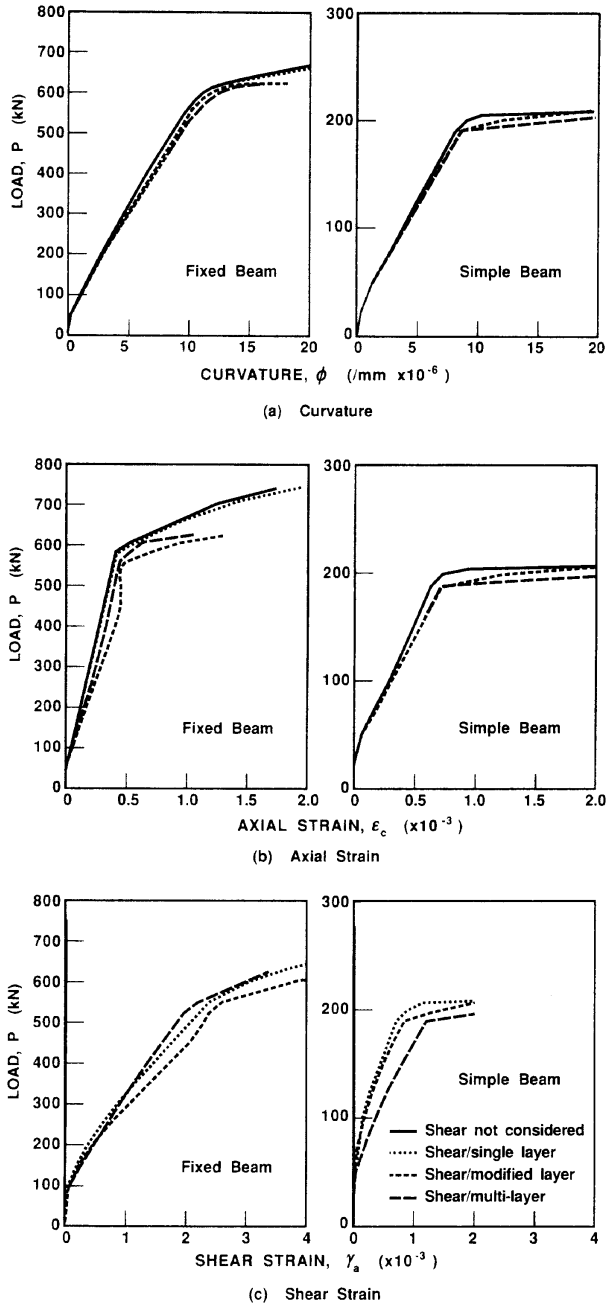

Fig. 3 — Comparisons of predicted sectional response

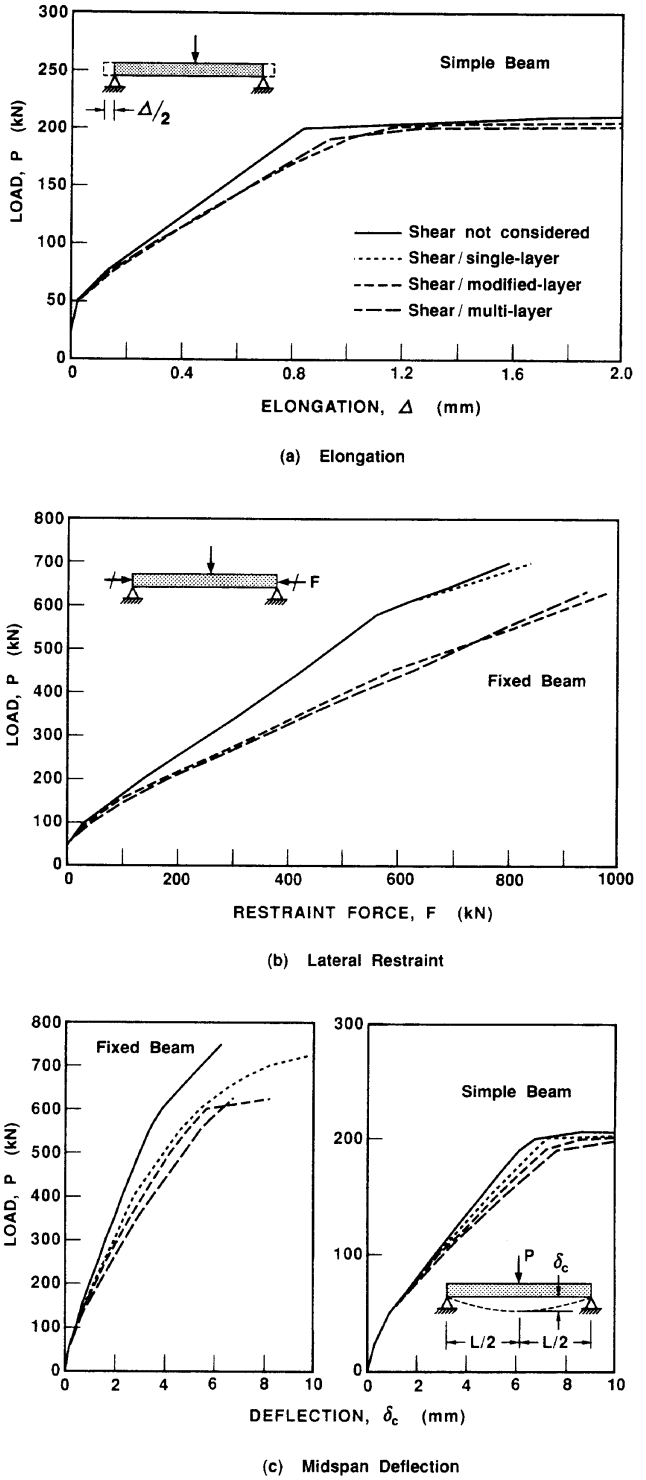

Fig. 4 — Comparisons of predicted member response

compared to the single-layer method, due to the influence of generally higher axial strains and curvatures (i.e. the middle layer is generally under higher axial tensile strain). Note too that in analyses where shear effects are not considered, no shear strain is predicted.

The influences just discussed relate to conditions at a single section and will vary with position. When combined and integrated over the length of the beams, they result in significant deviations in computed response. The total axial expansion of the simple beam, predicted using the various procedures, is shown in Fig. 4(a); the predicted lateral restraint force developed at the supports of the fixed-end beam is given in Fig. 4(b). Note that significantly higher axial displacements or axial restraint forces are developed when shear is taken into account. It is also important to note that the modified-layer procedure captures these influences very well in comparison to the multilayer procedure. Except near ultimate load conditions, where geometric nonlinearity effects are becoming more significant, the single-layer procedure provides a computed response identical to that obtained if shear effects are ignored.

The influence of shear on axial, flexural, and transverse strains is perhaps best reflected in the computed deflections. Fig. 4(c) shows the midspan deflections predicted for both beams. It is clearly evident that shear force effects result in a very significant increase in de-

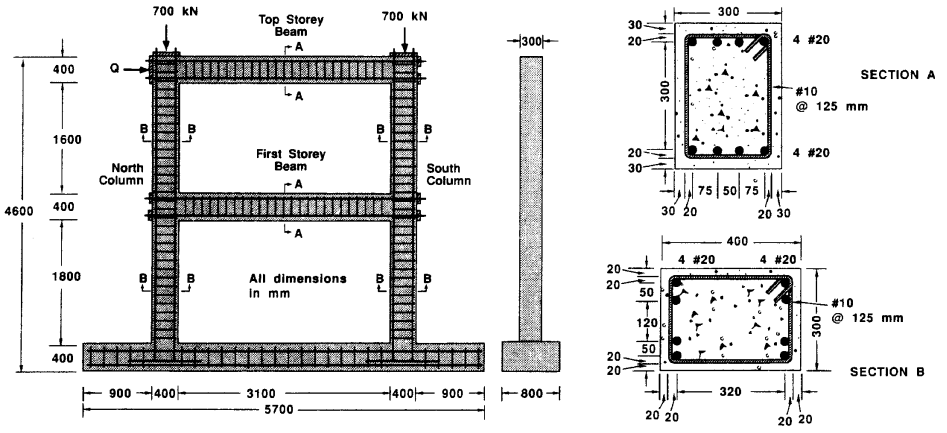

Fig. 5 — Details of test frame

flections, with the influence increasing at higher load levels. The modified-layer procedure captures much of this influence, generally accounting for about two-thirds to three-fourths of the increase in deflection due to shear. The discrepancy is related primarily to differences in the computed shear strains. The single-layer procedure captures only about one-third to one-half of the increase in deflection due to shear. In addition to incorrectly estimating shear strains, the single-layer procedure does not adequately account for the reductions in flexural stiffness due to shear-related effects.

The predicted ultimate load capacity and failure mode of the beams, as influenced by the manner in which shear effects are considered, are also of interest. In the case of the simply supported beam, an ultimate load of 205 kN (46 kip) is predicted if shear is not considered or if it is considered using either of the two single-layer procedures. The multi-layer procedure results in a slight lowering of the load capacity to 200 kN (45 kips), due to increased stresses in the longitudinal reinforcement. In all cases, the failure mode is of a ductile nature due to yielding of the reinforcement at the midspan. In the fixed-end beam, however, the influences are much more pronounced. If shear is not considered, the beam is computed to have an ultimate load capacity of 750 kN (169 kips), with a brittle flexural failure due to crushing of the concrete at the supports and at the midspan. Accounting for shear using the single-layer procedure reduces the load capacity to about 725 kN (163 kips). However, failure is found to be governed by a shear failure of the concrete near the supports. The multi-layer and modified-layer analysis procedures both result in the significantly reduced predicted load capacity of 625 kN (140 kips). The predicted failure mechanism becomes one involving a brittle flexural/shear failure due to concrete crushing.

EXPERIMENTAL INVESTIGATION

An experimental investigation was undertaken to corroborate the analytical work and lend further insight into the nature of shear deformations in frame structures. The test model chosen for study was the large-scale, one-span, two-story plane frame shown in Fig. 5. The frame was designed with a center-to-center span of 3500 mm (7 ft, 5 in.), a story height of 2000 mm (4 ft, 3 in.), and an overall height of 4600 mm (9 ft, 9 in.). All frame members were 300 mm (12 in.) wide by 400 mm (16 in.) deep. The frame was built integral with a large, heavily reinforced concrete base.

All members of the frame were similarly reinforced with four No. 20 deformed bars as bottom reinforcement, four No. 20 bars as top reinforcement, and No. 10 closed stirrups at 125 mm (5 in.) spacing as shear reinforcement. (Note that the nominal cross-sectional area of a No. 20 bar is 300 mm^2; of a No. 10 bar, 100 mm^2). Placement of the reinforcement was such as to provide a clear cover of 30 mm (1.2 in.) for the beams and 20 mm (0.8 in.) for the columns. Section details are given in Fig. 5. Note that the longitudinal reinforcement was anchored at all ends of members by welding the bars to stiff bearing plates.

The frame was formed and cast in a reclined position, using a low-slump ready-mix concrete with superplasticizer added. After a 14-day curing period, the formwork was removed and the frame was lifted to its upright position. The base of the frame was then bolted to the laboratory strong-floor, thus giving an essentially fully fixed condition at the column bases.

The concrete material properties were determined, on the test date, from 150 x 300 mm (6 x 12 in.) standard cylinders. The cylinder tests were conducted in a stiff testing machine, in stroke control mode, using a stroke rate of 4.0 x 10^{-3} mm/sec. The concrete was found to have a compressive strength of 30 MPa (4350 psi) and a stress-strain curve, as shown in Fig. 6(a).

The material properties of the No. 20 reinforcing steel, used as longitudinal reinforcement in all members, were determined from 300 mm (12 in.) coupons tested at a stroke rate of 5.6 x 10^{-3} mm/sec. Assuming a nominal cross-sectional area of 300 mm^2 (0.46 in.^{2}), the reinforcing steel bar was found to have a yield stress of 418 MPa (60 ksi), an ultimate stress of 596 MPa (86 ksi), and a modulus of elasticity of 192,500 MPa (27,900 ksi). A typical stress-strain curve is shown in Fig. 6(b). Note that the bars exhibited a rather short

yield plateau, terminating at a strain of about 9.5 x 10^{-3} mm/mm. The strain-hardening modulus observed thereafter had an average value of 3100 MPa (450 ksi). The No. 10 bars used for shear reinforcement had a yield strength of 454 MPa (66 ksi) and an ultimate stress of 640 MPa (93 ksi).

Testing of the frame model was to involve the case of constant axial loads applied to the columns combined with monotonically increasing lateral load applied at the top beam level. The test setup devised accordingly is illustrated in Fig. 7. The column loads were provided by four 450 kN (100 kips) capacity hydraulic jacks (two per column). The jacks, anchored to the strong-floor, were connected to transverse loading beams positioned across the top of the columns. The lateral load was supplied by a 1000 kN (220 kip) servocontrolled actuator reacting against a strong-wall. The base of the frame was post-tensioned against the strong-floor to prevent slip.

The test frame was extensively instrumented to monitor behavior during testing. Displacement transducers (LVDTs), placed at various points around the frame, were used to monitor deflections. Measurements of surface strain were made using electronic demountable gages (i.e., "Zurich" gages) from target points placed in a 300 mm grid pattern along each member. These provided measurements of longitudinal, transverse, and shear strains. Electrical resistance strain gages, applied to the reinforcement at various locations, were used to measure reinforcing bar strains. Load cells integrated with the jacks and actuator provided a measure of the applied load. Continuous monitoring and recording of data was accomplished using a computer-controlled scanning system.

The testing sequence involved first applying a total axial load of 700 kN (157 kips) to each column and maintaining this load in a force-controlled mode throughout the test. Lateral load was then monotonically applied, in a stroke-controlled mode, until the ultimate capacity of the frame was achieved. Discrete load stages were defined where lateral loading (i.e., displacement) was held constant while surface strain measurements were taken, crack patterns recorded, and visual inspections made. The load stages were initially set at approximately 25 kN (5.6 kips) load increments, reduced to 10 kN (2.25 kip) at intermediate stages of the test. In the latter stages, the load stages were defined by stroke increments. Testing continued over several days. At the end of each day, the frame was unloaded and residual conditions were recorded. The following day, the initial load stage would be at a load level approximately equal to the final load achieved the previous day.

It is important to note that, as the frame deflected laterally under increasing load, the column loads deviated from vertical. Thus, the total lateral load applied to the frame included counteracting horizontal force components arising from the column loads, albeit small. The horizontal forces reported hereafter have been adjusted accordingly.

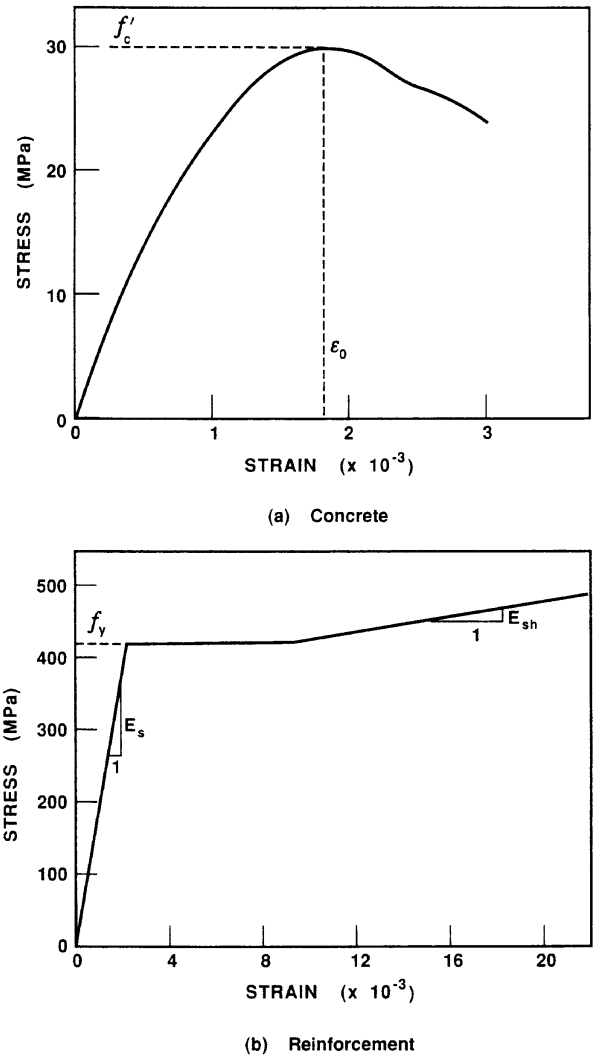

Fig. 6 — Material stress-strain properties

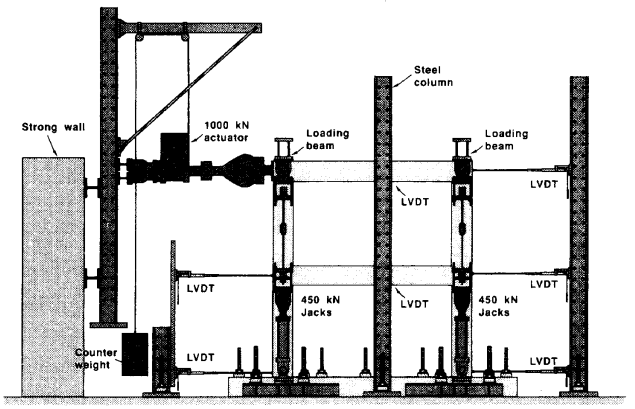

Fig. 7 — Test setup

TEST OBSERVATIONS

The overall load-deformation response of the test frame is summarized in Fig. 8. The measured lateral displacement is plotted at the top of the frame versus the applied lateral load. Key load stages in the test are indicated.

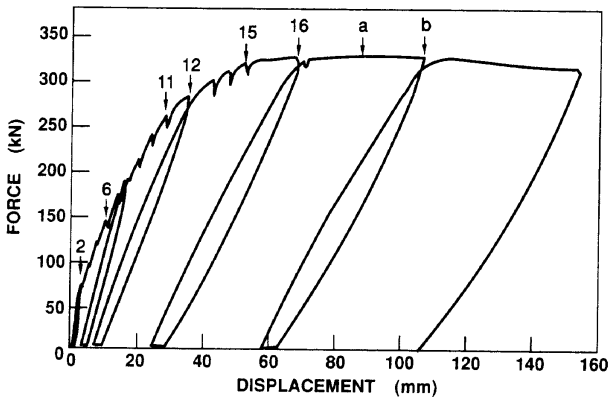

Fig. 8 — Test history in terms of applied lateral load versus deflection at top story

(a) Frame at Ultimate Load

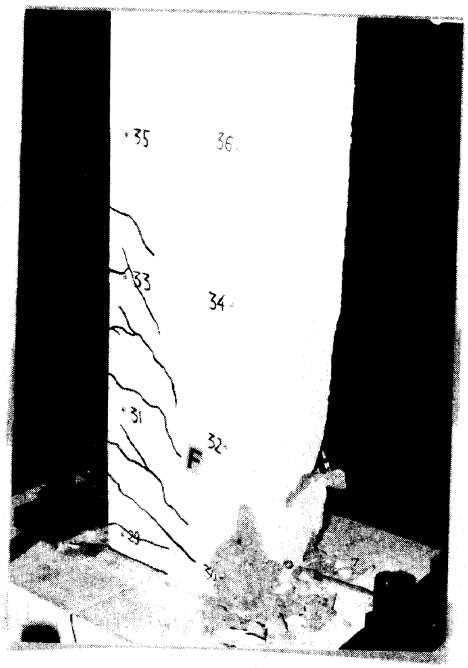

(b) Base of South Column

Fig. 9 — Views of test frame at ultimate load

The frame experienced first cracking at a load of 52.5 kN [load stage (LS) 2]; flexural cracks were observed in the first-story beam at the north bottom face and at the south top face. The first apparent decrease in the stiffness of the load-deformation response was evident at this time. Flexural cracking at the base of the columns occurred at a load of 145 kN (LS6). At this load, the first web-shear cracks in the first-story beam were also detected. Thereafter, the response of the structure became progressively softer as cracking propagated throughout all members.

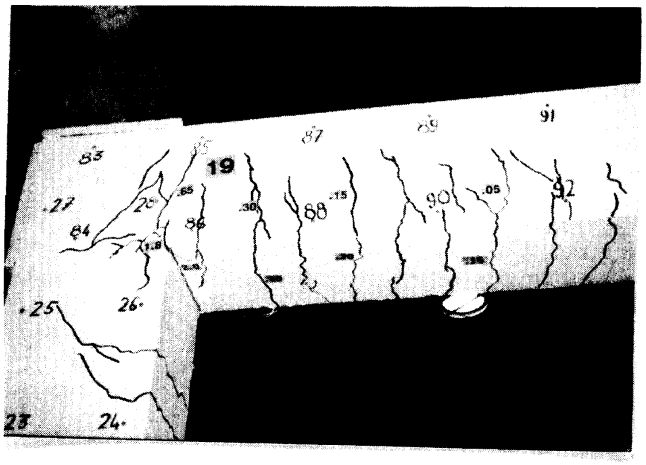

(c) North-Top Joint

Fig. 9 — View of test frame at ultimate load.

At a load of 264 kN (LS11), strain gages indicated that first yielding occurred in the bottom longitudinal reinforcement at the north end of the first-story beam. Yielding in the top reinforcement at the south end of the beam occurred shortly after, at a load of 287 kN (LS 12). This resulted in a perceptible drop in the frame's lateral stiffness. Yielding at the base of both columns, and hinging (i.e., yielding of both compression and tension reinforcement and concrete crushing) at both ends of the first-story beam occurred as the load approached 323 kN (LS 15). Shortly after, at a load of 329 kN (LS 16), concrete crushing and hinging was evident at the base of the columns. At about the same time, yielding and hinging developed at both ends of the top-story beam. The stiffness of the load-deformation response decayed rapidly, but the frame demonstrated excellent ductility after achieving ultimate load. Loading was terminated at a lateral displacement of about 150 mm (6 in.), due to the stroke limitations of the actuator.

The frame sustained an ultimate lateral load of 332 kN (75 kips) at a lateral drift of 2.0 percent. The failure mechanism involved ductile hinging at the ends of the beams and at the bases of the columns, with the hinges forming in quick succession as ultimate load was approached. While some shear cracking was observed in the beams and in the columns, the failure mode in each member was predominantly flexural. Moreover, secondary moment effects (i.e., $P-\Delta$ effect) had significant influence on the capacity of the structure, accounting for about 12 percent of the total overturning moment acting on the structure at ultimate. Shown in Fig. 9 is the condition of the structure at ultimate load.

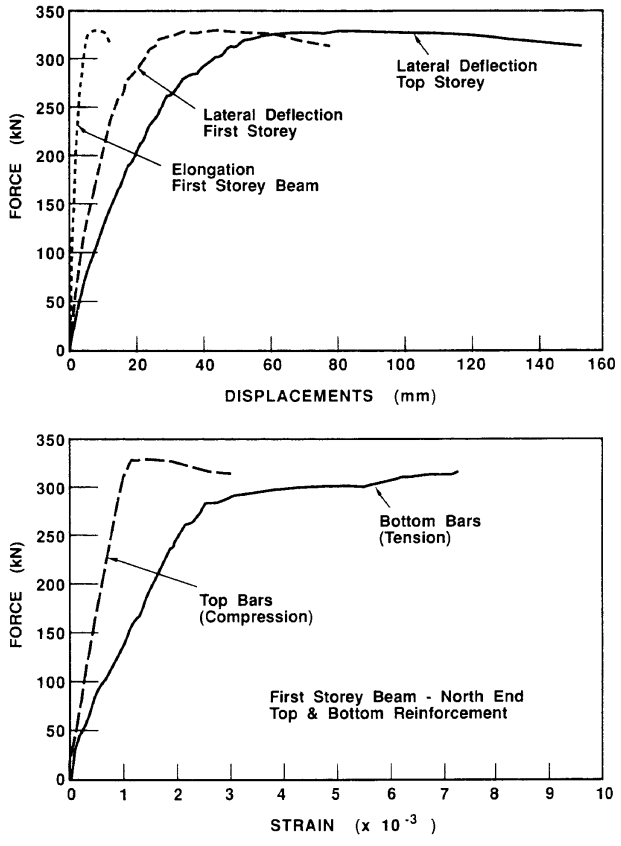

Fig. 10 — Response of test frame

Some representative data describing the response observed are given in Fig. 10.

Of particular interest in this test was the magnitude and influence of the shear deformations in the frame. Fig. 11 shows the transverse shear strains, computed from the Zurich strain readings, at various points in the structure. Although failure was primarily flexural in nature, the shear strains are seen to have been of significant magnitude, particularly in later load stages. Relatively high shear strains were observed at the base of the north column, at the north end of the second-story beam, and at both ends of the first-story beam. By comparison, the shear strains measured in the south column were relatively smaller, due to the effects of higher axial compression. It is also interesting to note that the highest shear strains were observed in the top-story, north beam-column joint. This is consistent with the observation of large diagonal cracks in this region [see Fig. 9(c)].

From the shear strains measured, it is possible to surmise that direct shear deformation of the columns contributed a significant amount to the total lateral displacement of the frame. At an average shear strain of 1.5×10^{-3} mm/mm at ultimate load, the shear deflection over the length of the columns would be 6.0 mm (0.25 in.), or about 10 percent of the total lateral deflection measured. More important, perhaps, is that the large shear deformations in the beams, and the added deterioration of flexural stiffness in all members due to shear stresses, further reduced the lateral stiffness of the structure.

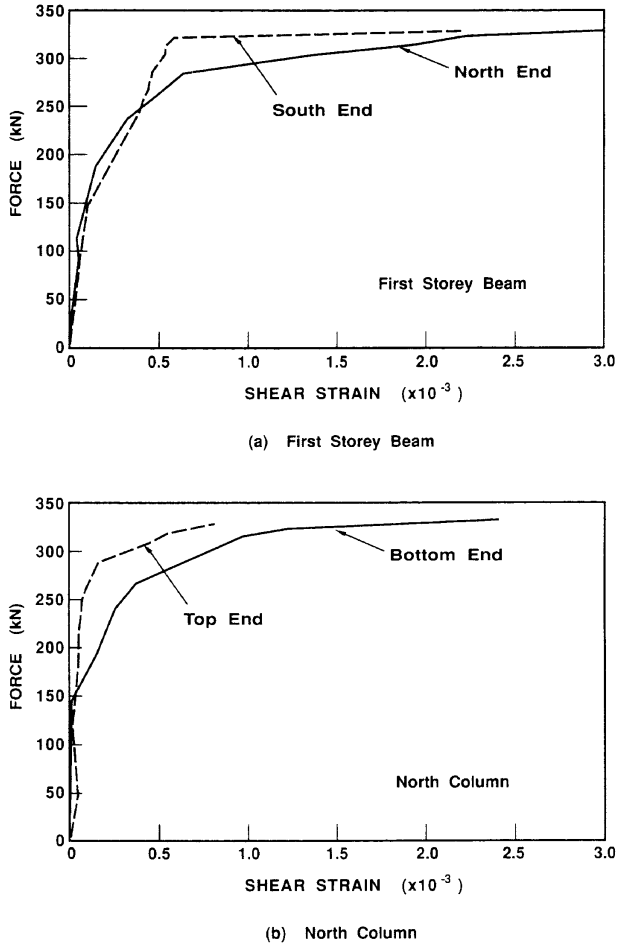

Fig. 11 — Measured shear strains in frame members

PREDICTED RESPONSE

Theoretical predictions of the response of the test frame were obtained using the computer program TEMPEST, modified to include shear effects in the manner previously described. The computer model of the structure was formulated consistent with the test frame's geometry and reinforcement details. Forty member segments were used in the discretization; six for each column and eight for each beam. The column bases were assumed fully fixed, and the material properties used were as determined from cylinder or coupon tests. The analysis options selected included the consideration of material nonlinearity, geometric nonlinearity, tension stiffening, membrane action, and shear effects. Shear was considered using the multi-layer analysis approach.

The accurate prediction of local (i.e., sectional) strain response of a frame member is critical to the analysis procedure. Fig. 12 compares the observed and predicted sectional strains at the base of the north column. It can be seen that the curvature, net axial strain, and normal shear strain are all modeled reasonably accurately. Similar degrees of correlation were found at other locations investigated.

Comparisons of some aspects of the overall response of the test frame are made in Fig. 13. Fig. 13(a) compares the load-deflection response at the top-story beam level. The gradually softening deflection response is

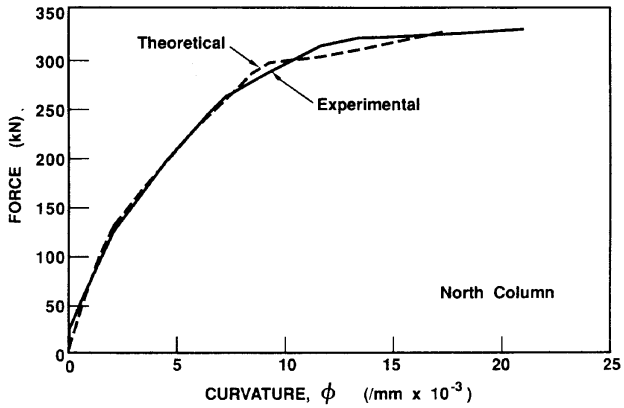

(a) Curvature

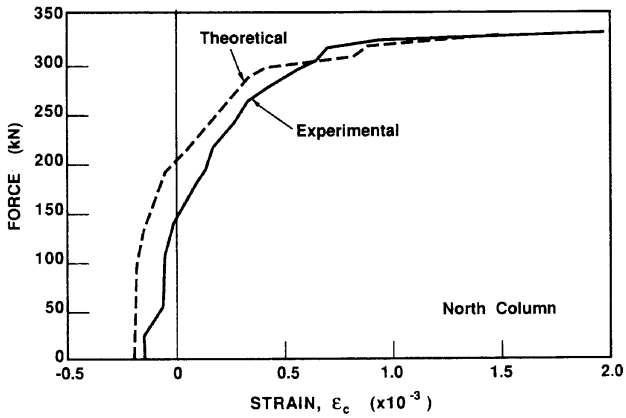

(b) Axial Strain

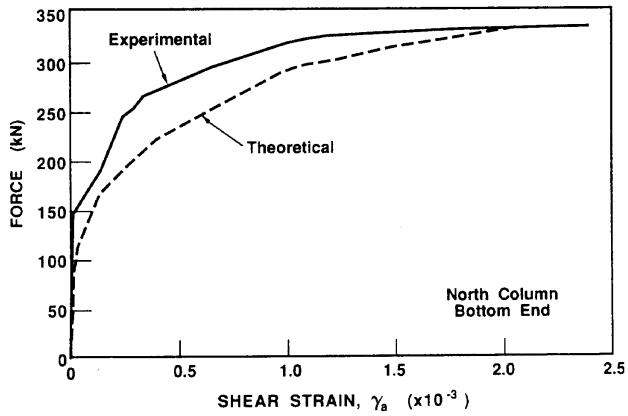

(c) Shear Strain

Fig. 12 — Comparisons of predicted and observed sectional responses

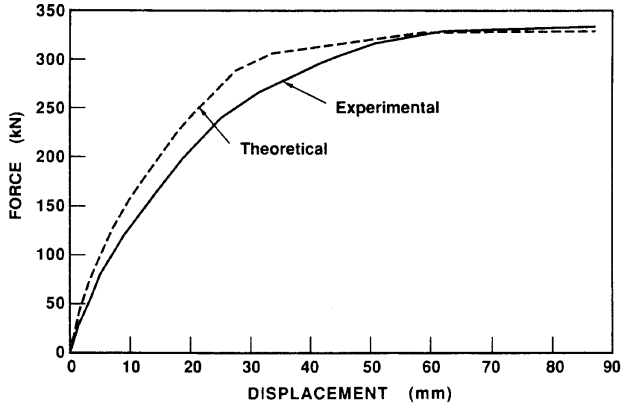

(a) Lateral Deflections at Top Storey

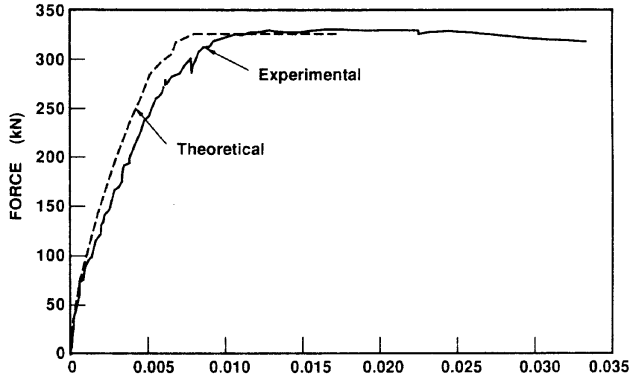

(b) Rotation at Top-North Joint

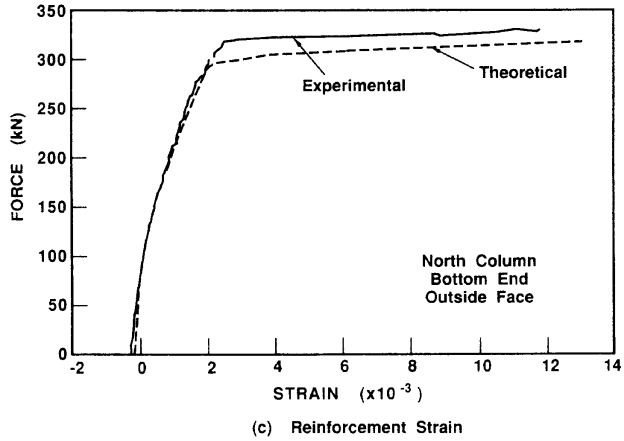

(c) Reinforcement Strain

Fig. 13 — Comparisons of predicted and observed overall frame response

simulated reasonably well, although the theoretical response tends to be somewhat stiffer. The greater flexibility observed in the test structure could possibly be attributable to the effects of shrinkage stresses, concentrated deformations in the joints, or slight rotation at the base of the columns due to bond slip. Nevertheless, the ultimate load capacity is predicted fairly accurately, with the computed value of 328 kN (74 kips) corresponding to 98.8 percent of the observed strength. Other aspects of overall frame response were also predicted well; for example, rotation at the top-north joint [Fig. 13(b)], and strains in the reinforcement [e.g., Fig. 13(c)]. Not apparent in the response curves, but equally important, is that behaviorial aspects such as local yielding and hinging and the sequence of formation of the collapse mechanism were also well simulated. For example, the formation of the plastic hinge at the base of the south column was predicted to occur at a load of between 308 kN and 318 kN; experimental evidence suggests that it occurred at about 326 kN.

It would be of interest to determine the degree to which the theoretical response was influenced by shear effects. Fig. 14 shows the displacement at the top story

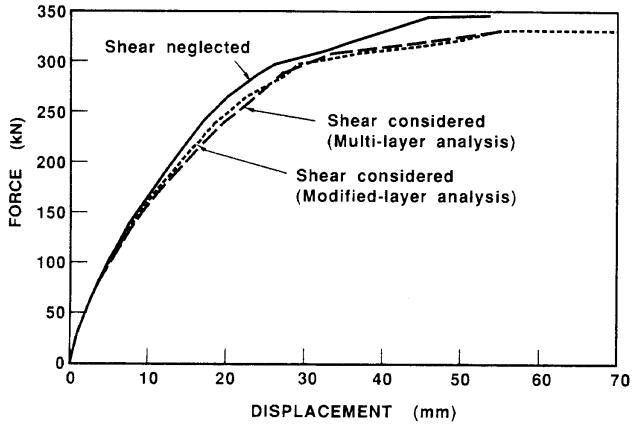

Fig. 14 — Theoretical influence of shear on lateral deformation of frame

as variously predicted using the rigorous multi-layer analysis, the modified-layer analysis, and by ignoring shear altogether. It can be seen that the influence of shear resulted in a significant increase in the flexibility of the structure, particularly near ultimate loads where deflections were increased by as much as 20 percent. A slight decrease in the load capacity was also brought about. The approximate modified-layer analysis was able to capture to a large extent this influence.

Also of interest would be a comparison between the computed nonlinear response and that obtained from conventional analyses. A linear elastic analysis of the test structure was made assuming effective stiffnesses of 0.5 I_g for the beams and 1.0 I_g for the columns. Shown in Fig. 15 are the lateral deflections and column base shears determined accordingly. It can be seen that the linear elastic analysis significantly underestimates deflections, even at service load levels. Also, no consideration is given to the significant redistribution of base shears that occurs among the columns, as predicted by the nonlinear analysis. The redistribution of base shear is a result of axial expansion of the beams and a more rapidly decaying stiffness in the north column.

CONCLUSION

An analytical procedure was described whereby the influence of shear-related effects on the strength and deformation response of reinforced concrete frames can be modeled. This procedure was used in a theoretical study of the nature, magnitude, and influence of shear effects in frame members. As well, a large-scale frame model was tested to corroborate the analytical formulation and to provide further insight into the influence of shear effects.

Shear is found to contribute to the deformation of a frame under load by various direct and indirect means. Transverse shear strains developed in frame members directly reduce the lateral stiffness of a frame. However, shear stresses also act to reduce the flexural and axial rigidity of members, increasing their rotational and axial straining and thereby further increasing frame

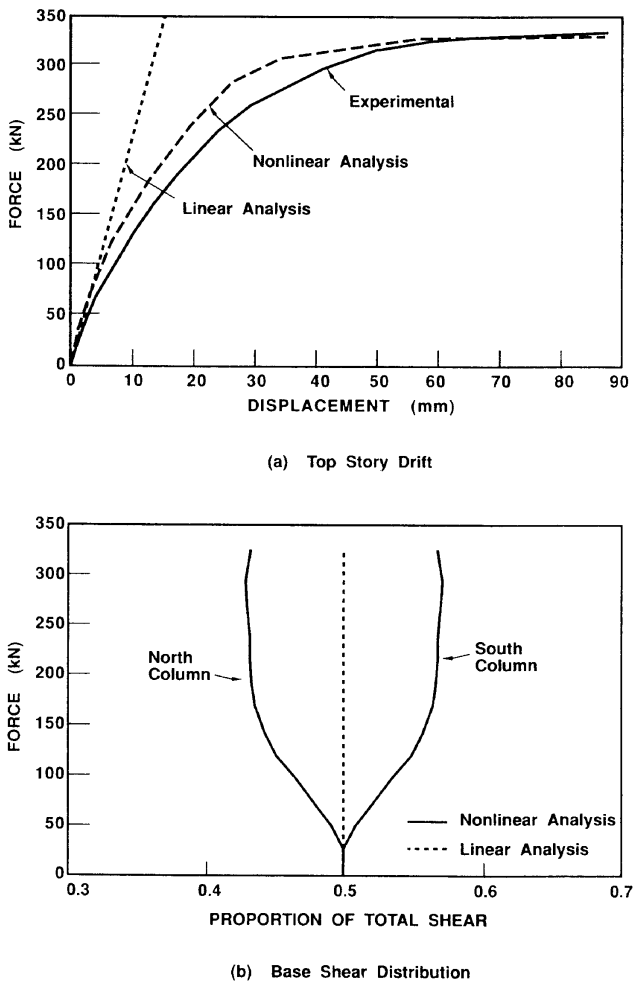

Fig. 15 — Comparisons between linear and nonlinear analyses

displacements. The ultimate load and failure mechanism of the frame can be affected as a result of increased deflections (e.g., P-Δ effects) or because of deteriorated material strength (e.g., concrete shear/crushing).

The theoretical and experimental investigations both indicated that shear-related deformations can represent a significant portion of the total deflection in a frame. The magnitude will vary depending on the frame geometry, loading condition, and load level. In the frame investigated herein, the shear-related contribution to the total deflection was in the range of 20 percent despite a predominantly flexural failure mode. This influence can be greater in structures governed by shear failure.

The analytical procedure developed, based on a multilayer two-dimensional stress analysis method for beam sections integrated into a nonlinear frame analysis algorithm, is found to provide reasonably accurate predictions of response. The load-deformation response, ultimate load capacity, and failure mechanism of a frame, as well as the local sectional behaviors, can be predicted reasonably well.

An approximate analysis, based on a modified-layer method accounting for shear-related reductions in axial and flexural stiffness and for transverse shear strains,

will give reasonably accurate predictions approaching those of the more rigorous multilayer analysis. An single-layer analysis, accounting for only shear-strain effects, will give generally poor results.

ACKNOWLEDGMENT

The work presented in this paper was made possible through funding from the Natural Sciences and Engineering Research Council of Canada. The authors wish to express their sincrere gratitude for the support received.

CONVERSION FACTORS

1 mm = 0.039 in.
1 kN = 0.225 kips

REFERENCES

1. Vecchio, F. J., "Nonlinear Analysis of Reinforced Concrete Frames Subjected to Thermal and Mechanical Loads," *ACI Structural Journal,* V. 84, No. 6, Nov.-Dec. 1987, pp. 492-501.

2. Vecchio, F. J., and Sato, J. A., "Thermal Gradient Effects in Reinforced Concrete Frame Structures," *ACI Structural Journal,* V. 87, No. 3, May-June 1990, pp. 262-275.

3. Vecchio, F. J., and Tang, K., "Membrane Action in Reinforced Concrete Slabs," *Canadian Journal of Civil Engineering,* V. 17, No. 5, Oct. 1990, pp. 686-697.

4. Vecchio, F. J., and Balopoulou, S., "On the Nonlinear Behaviour of Reinforced Concrete Frames," *Canadian Journal of Civil Enginering,* V. 17, No. 5, Oct. 1990, pp. 698-704.

5. Vecchio, F. J., and Collins, M. P., "Predicting the Response of Reinforced Concrete Beams Subjected to Shear Using the Modified Compression Field Theory," *ACI Structural Journal,* V. 85, No. 3, May-June 1988, pp. 258-268.

6. Vecchio, F. J., and Collins, M. P., "Modified Compression Field Theory for Reinforced Concrete Elements Subjected to Shear," ACI JOURNAL, *Proceedings* V. 83, No. 2, Mar.-Apr. 1986, pp. 219-231.

7. Adebar, P., "Shear Design of Concrete Offshore Structures," PhD thesis, Department of Civil Engineering, University of Toronto, 1989, 197 pp.